Asian Journal of Chemistry; Vol. 32, No. 3 (2020), 646-652

ASIAN JOURNAL OF CHEMISTRY

https://doi.org/10.14233/ajchem.2020.22469

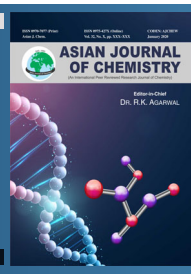

Theoretical Verification of Dielectric and Magnetic Properties of Polyaniline-Nickel Ferrite Nanocomposites Synthesized in Green Medium Extracted from the Fruit of *Tamarindus indica*

T.R. SMITHA[1], THUSHARA BHADRAN[2], VAISHALI SHANKER[2] and K.H. PREMA[2,*]

[1]Department of Chemistry, T.K.M.M. College (Affiliated to University of Kerala), Nangiarkulangara-690513, India
[2]Department of Chemistry, Santana Dharma College (Affiliated to University of Kerala), Alappuzha-688003, India

*Corresponding author: E-mail: premakh@gmail.com

Received: 27 September 2019; *Accepted*: 12 November 2019; *Published online*: 31 January 2020; AJC-19773

Nanocomposite materials of nickel ferrite incorporated polyaniline (PANI) have been synthesized *via in situ* oxidative polymerization technique in a green medium extracted from the fruit of plant *Tamarindus indica*. Synthesized particles were characterized by FT-IR spectroscopy, X-ray diffraction technique and scanning electron microscopy. Various samples of composites were prepared with 5, 10 and 15 g of filler nickel ferrite and the variation in dielectric permittivity is calculated by measuring the capacitance of the materials in various external frequency ranges from 100 Hz to 20 MHz. Experimental values of dielectric property are compared with theoretical values obtained from Maxwell-Wagner equation. The magnetic properties such as saturation magnetization (Ms), magnetic remanance (Mr) and coercivity (Hc) of the samples were analyzed by vibrating sample magnetometer (VSM). Retention of the magnetic filler in the PANI matrix is evaluated by comparing the experimental Ms values of the composites with the values computed from a theoretical linear equation. The experimental results were well fitted with the theoretical values and confirmed the synthesis of PANI-nickel ferrite composites with desired electrical and magnetic properties by varying the amount of components.

Keywords: *Tamarindus indica*, Nanocomposites, Dielectric property, Maxwell-Wagner equation, VSM analysis.

INTRODUCTION

Polymer-ferrite nanocomposite materials have been established as common materials in the field of electronics. Their unique properties with electronic conductivity in the semiconducting region comprising the magnetic properties gave them a promising space in the area of technology [1-3]. These materials find technological applications such as bio-sensors, electromagnetic absorbers, magnetic recording tapes, electro catalysts, photo electronic devices and magnetic pigments. Properties of these materials can be tuned by varying the amount of requisite materials. Materialists are very conscious to extend the range of magnetic filler with transition and inner transition elements. Researchers focused on the synthesis of PANI-composites in protonic acids such as HCl, H_2SO_4, HNO_3, *etc*. [4-8]. A green medium for the synthesis of PANI-composites is not yet introduced. Studies reported that synthesis of PANI-composites in mineral acids may affect the magnetic ferrite filler. In this context the present study aims to synthesize polyaniline-ferrite composites with nickel ferrite filler in a green medium tamarind extract, which is a good source of tartaric acid.

Among the organic molecules having electronic property polyaniline attract the attention due its low cost of production, easy method of formulation and wide range of applicability. It has been reported that polyaniline exists in three stable and isolable oxidation states – leuco-emeraldine (fully reduced), emeraldine (half oxidized) and pernigraniline (fully oxidized) where the value of 1-y becomes 0, 0.5 and 1, respectively and are represented in the Fig. 1. PANI possesses controlled conductivity within the range of 10^{-10} to 10^{1} S cm^{-1}. Electronic properties of this organic polymer debt to conjugated π-electrons present on its backbone. The conductivity of these materials can be tuned by chemical manipulation of the polymer backbone, by the nature of the dopant, by the degree of doping, pH of the solvent and by blending with other polymers [9-12]. Conductivity of polyaniline is due to the protonation of imine N-atoms which results the formation of corresponding salts.

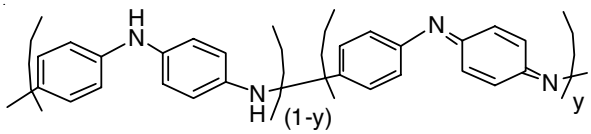

y=0, Leuco-emeraldine; y=0.5, Emeraldine; y=1, Pernigraniline

Fig. 1. Different oxidation states of PANI

Among the three oxidation states, emeraldine salt is the only conductive form PANI. Non-conductive emeraldine base form can be converted to the conductive salt form by the process called doping. Protonation of PANI is referred to as doping which may be done during the oxidative chemical polymerization reaction [13-17].

Ferrites are mixed metal oxides with Fe^{3+} as their main component and are classified in to spinel ferrites, garnet ferrites and hexagonal ferrites based on their crystal structure. Spinel ferrites have the general chemical formula $(MFe_2O_4)_n$, where M represents a divalent metallic cation. In the spinel unit cell, 32 oxygen anions form a close packed cubic structure which encloses 96 interstices, 64 tetrahedral (A site) and 32 octahedral (B site). Among these 24 sites are occupied by cations. Based on the distribution of Fe and M cations in the A and B sites ferrites are categorized in to normal spinels (M ions occupy A sites and Fe ions occupy the B sites), inverse spinels (M ions occupy B sites and Fe ions equally accommodate in A and B sites) and random spinels (both M and Fe ions occur in A and B sites). The unique magnetic and electrical properties of ferrites depend on the distribution of M^{2+} and Fe^{3+} ions in the A and B sites. The main factor influencing the cation occupancy in A and B sites of ferrites is crystal field stabilization energy (CFSE). Fe^{3+} has no CFSE and no site preference and therefore CFSE and site preference of divalent cations define the structure of ferrites. In the case of nickel ferrite, nickel ion acquires more CFSE in octahedral site than tetrahedral site and therefore occupies in the B site and thus forms an inverse spinel structure. Magnetic properties of ferrites depend on the distribution of cations in the interstitial sites A and B. Negative interaction energies of adjacent sites result antiparallel orientation of spins. Net magnetic moment is the difference of magnetic moments between A site and B site ions. Ni^{2+} ion possesses two unpaired electrons responsible for magnetic property. Another important property shown by ferrite is hysteresis, retention of magnetism in the absence of external magnetic field. The properties of a magnetic material can be explained from the values of saturation magnetization (Ms), coercive force (Hc). Ms is the maximum magnetic dipole moment per unit volume, Mr is the magnetic domains remain on removal of the external field and Hc is the reversed applied field to reduce the magnetic flux to zero. Ferrites with high value of coercivity are known as hard ferrites and with low coercivity are known as soft ferrites. Hard ferrites resist demagnetization and soft ferrites can easily demagnetize without dispersing much energy. Nickel ferrite is under the category of soft ferrite [18,19].

Green synthesis emphasizes the use of natural resources in place of laboratory chemicals, reduction or prevention of the use of toxic chemicals and reduction of the formation of dangerous byproducts. Moreover it ensures the production of environmentally friendly, economic and biocompatible products. Green methods take a vital role in the synthesis of nanoparticles. Tamarind is a long living branched tree with native to tropical Africa. Long ago it is introduced in India and therefore it is reported that tamarind is indigenous to India also. It is a very common plant in Kerala. It produces a pod like fruit which contains a brown pulpy mass with seeds inside). Ripening of the green tamarind fruits takes place in the months April to June. The fruits will fall naturally when they ripe. A well grown tree may produce about 150 to 225 kg of fruits annually with 30 to 55 % of pulp. The sun-dried pulp can be stored for several years by mixing with 10 % salt. It is reported that the tamarind pulp is a promising source of tartaric acid. Extract of pulp with water is called tamarind syrup which is found to be acidic in nature. The present work is to evaluate the effectiveness of the green medium for the synthesis of PANI-ferrite composite.

EXPERIMENTAL

Analytical grade ferric nitrate and nickel nitrate were purchased from Qualigens chemicals with 98 % purity. Aniline and acetone used for the synthesis of polyaniline were purchased from Merck chemical company and ammonium peroxydisulphate from Spectrochem and all are of high purity. Aniline is used after double distillation. 30 g tamarind fruit, squeezed with 250 mL distilled water and filtered tamarind extract at pH 2.

Synthesis of nickel ferrite ($NiFe_2O_4$): Ultrafine particles of nickel ferrite were prepared by sol-gel method using nickel nitrate $[Ni(NO_3)_2{\cdot}6H_2O]$ and ferric nitrate $[Fe(NO_3)_3{\cdot}9H_2O]$. Ferric nitrate and nickel nitrate are dissolved in pure ethylene glycol at 40 °C in the molar ratio 2:1. This solution is then heated to 60 °C and the temperature is kept constant till a wet gel of the metal nitrate is obtained. The gel is then dried at 100 °C to get nanoparticles of nickel nitrate. It was grinded and heated at 200 °C in a muffle furnace to get fine particles.

The chemical reaction leading to the formation of nickel ferrite is as follows:

$$Ni(NO_3)_2{\cdot}6H_2O + 2Fe(NO_3)_3{\cdot}9H_2O \longrightarrow NiFe_2O_4 + \text{volatilities}$$

Synthesis of PANI-nickel ferrite composites: Conductive PANI composites are synthesized by *in situ* oxidative chemical polymerization of aniline in green medium tamarind extract in the presence of ferrite particles. In the slow polymerization process PANI is allowed to form coating over ferrite particles.

Aniline monomer is dissolved in 100 mL tamarind extract at pH 2. Pre-synthesized ferrite (in varying amount) powder is added slowly to the reaction medium with vigorous stirring in order to keep ferrite powder suspended in the solution. To this ammonium persulphate solution in 50 mL tamarind extract with aniline/persulphate ratio 1:1.25 is added drop wise with continuous stirring. The reaction mixture is kept at 0-5 °C. Polymerization of aniline is allowed to takes place over fine graded ferrite particles. After the complete addition of the oxidant, the solution is kept undisturbed for 4-6 h. The resulting precipitate is filtered under suction, washed with distilled water and then with acetone. After washing, the precipitate is dried

in an air oven at 50 °C for 24 h. The obtained composite is grinded into a fine powder in smooth agate mortar in the presence of acetone medium.

Various samples of PANI-ferrite composites are prepared with 0.4 M aniline and 5, 10 and 15 g of filler nickel ferrite and are represented as P4N5, P4N10 and P4N15, respectively. (The weight fractions of filler in these compositions are 57.3, 72.8 and 80.12, respectively).

The FTIR spectra was recorded on a Thermo Nicolate Avatar370 (Model) spectrophotometer in KBr medium in the region 4000-400 cm^{-1} having DTGS detector. The phase analysis of the samples was carried out using Rigaku D max-B model X-ray diffractometer using Cu Ka radiations. SEM analysis of the samples is done with the SEM make JEOL Model JSM-6390LV. Room temperature magnetic measurements of the ferrite and PANI composites are carried out by VSM: model Lakeshore VSM 7410.

RESULTS AND DISCUSSION

X-ray diffractograms of PANI-$NiFe_2O_4$ composite: X-ray diffraction patterns of PANI, nickel ferrite and the composite P4N5 are shown in Fig. 2. All the characteristic peaks corresponding to the planes (220), (311), (400), (422), (611) and (440) are observed in the spectrum of nickel ferrite which agrees with the JCPDS no.80-0072 and confirms the formation of its spinel structure. Broad peaks of PANI at 2θ around 20° and 25° corresponding to (020) and (200) crystal planes ensures the formation of PANI in the emeraldine forms.

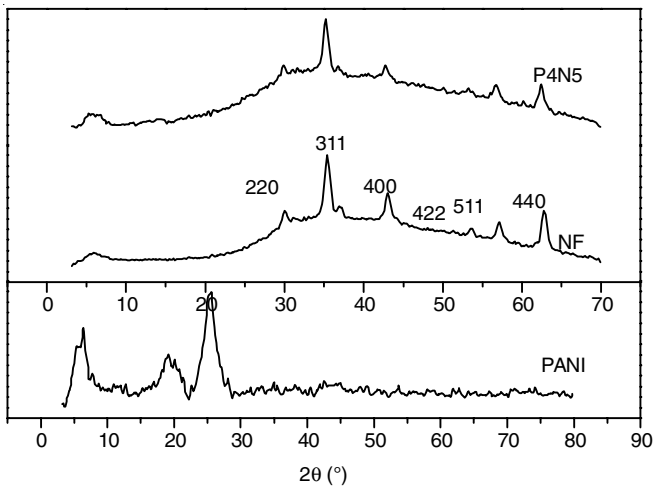

Fig. 2. XRD of nickel ferrite (NF), PANI and PANI-nickel ferrite composite (P4N5)

Retention of all the peaks due to ferrite along with the broad peak of PANI observed in the spectrum of the composite P4N5 ensures the presence of ferrite in the PANI matrix and that no structural change had occurred during the *in situ* polymerization of PANI in presence of nickel ferrite. Average particle size of nickel ferrite and P4N5 calculated using Debye-Scherrer formula are about 13 and 13.07 nm, respectively.

FT-IR studies: Fig. 3 shows the FTIR spectrum of nickel ferrite, PANI and P4N5. Tetrahedral and octahedral metal-oxygen vibrational peaks of nickel ferrite are observed at 555 and 637 cm^{-1}, respectively. PANI shows characteristic bands at around 1569, 1485, 1292, 1111 and 798 cm^{-1}. The bands appear at 1485 and 1569 cm^{-1} corresponding to C=C stretching vibrations of N-B-N (benzenoid) and N=Q=N (qunonoid) structures, respectively. Presence of these absorption bands confirms the formation of PANI in the most conductive emeraldine in the green medium. Absorption band at 798 cm^{-1} is due to out of plane bending vibration of C-H bond of 1,4-disubstituted benzene ring which confirms the conjugated π system present in PANI. A strong band appears at 1110 cm^{-1} has been explained as an in-plane bending vibration of imino-1,4-phenylene and has been reported to be associated with the electrical conductivity of PANI. P4N5 shows all the characteristic peaks of PANI and nickel ferrite and dispersion of ferrite in the PANI matrix is well proved.

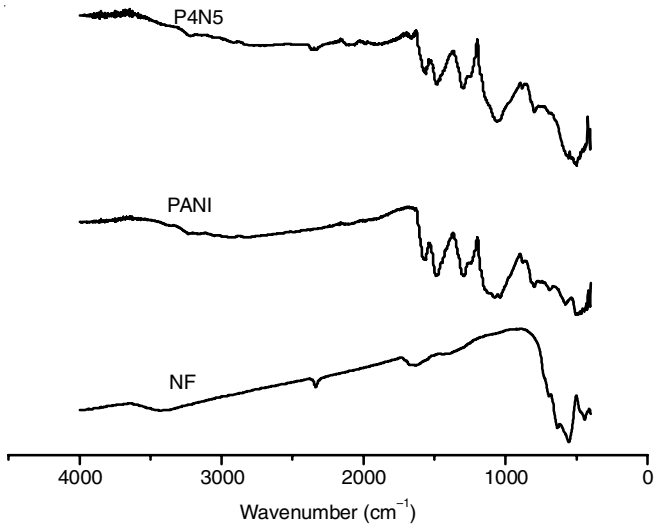

Fig. 3. FTIR spectrum of nickel ferrite (NF), PANI and PANI-nickel ferrite composite (P4N5)

SEM analysis: Fig. 4 represents the SEM micrographs of nickel ferrite, PANI and P4N5. Non-homogeneous distribution of ferrite particles is observed in the SEM of nickel ferrite. Agglomerated particles can also be observed. This may due to the magnetic properties of ferrite. Coating of PANI over ferrite can be observed in the SEM image of the composite.

Dielectric studies: The dielectric constant (ε) of a dielectric material is the ratio of the capacitance with that material as the dielectric in a capacitor to the capacitance when vacuum is used as the dielectric.

Dielectric constant (ε) is calculated from the equation, $\varepsilon = Ct/\varepsilon_0 A$, where, C = capacitance using the material as the dielectric in the capacitor, C_0 = capacitance using vacuum as the dielectric, ε_0 = dielectric permittivity of free space (8.854×10^{-12} F/m), A = sample cross sectional area, t = thickness of the sample.

Variation of dielectric permittivity of PANI, nickel ferrite and PANI-nickel ferrite composites with applied frequency are depicted in the Figs. 5-7. It is found that PANI shows high dielectric permittivity at low frequencies which decreases with the increase in frequency and reaches a constant value at high frequencies. Nickel ferrite and the composites also follow the same behaviour. Dielectric behaviour of a material under the influence of an external electric field depends on the polari-

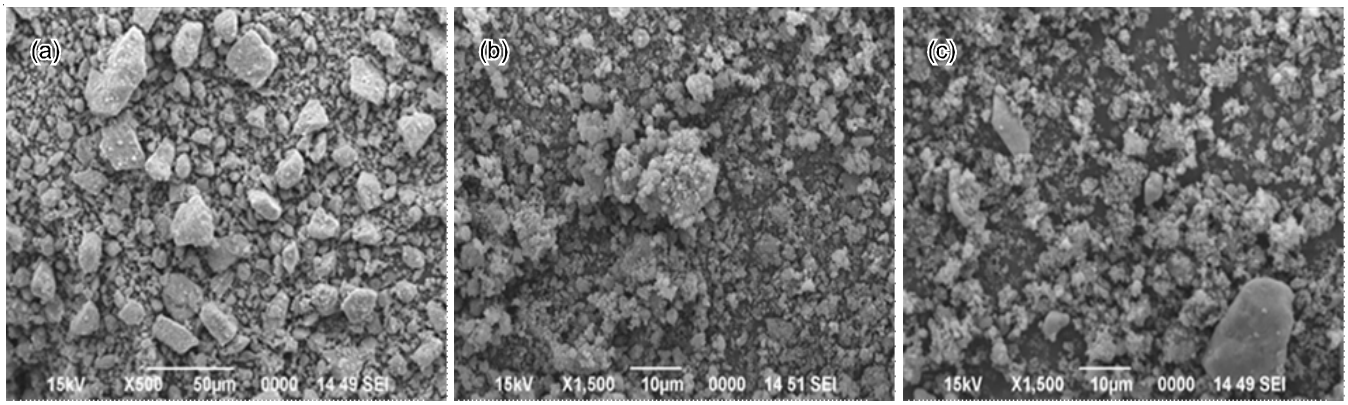

Fig. 4. SEM micrographs of (a) nickel ferrite, (b) PANI and (c) PANI-nickel ferrite composite

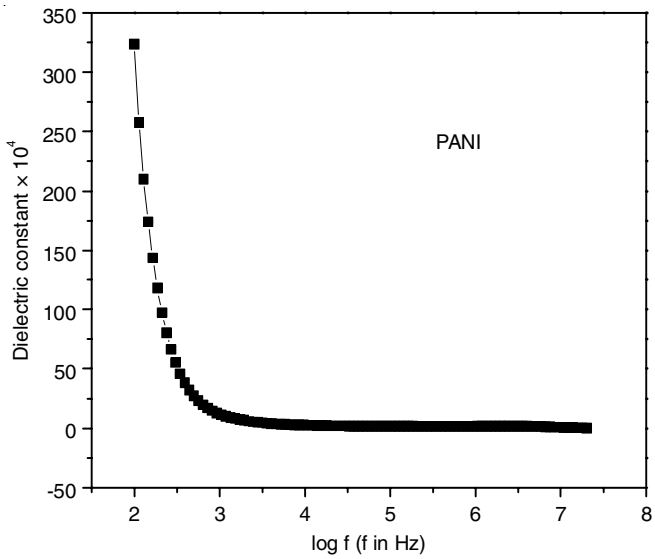

Fig. 5. Variation of dielectric permittivity of PANI with applied frequency

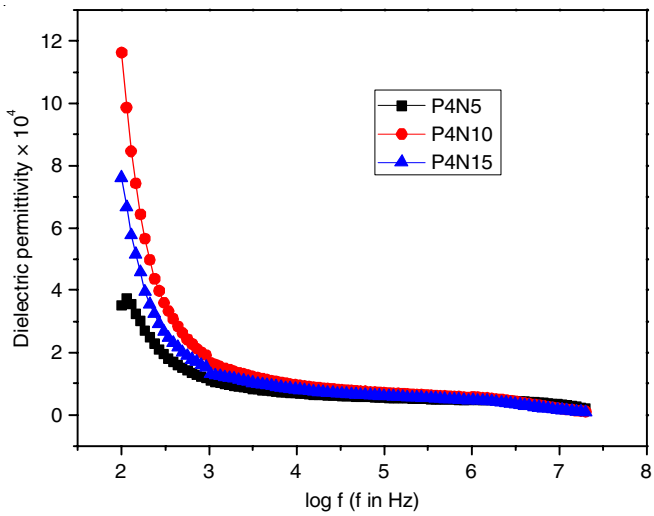

Fig. 7. Variation of dielectric permittivity of PANI-nickel ferrite composites with applied frequency

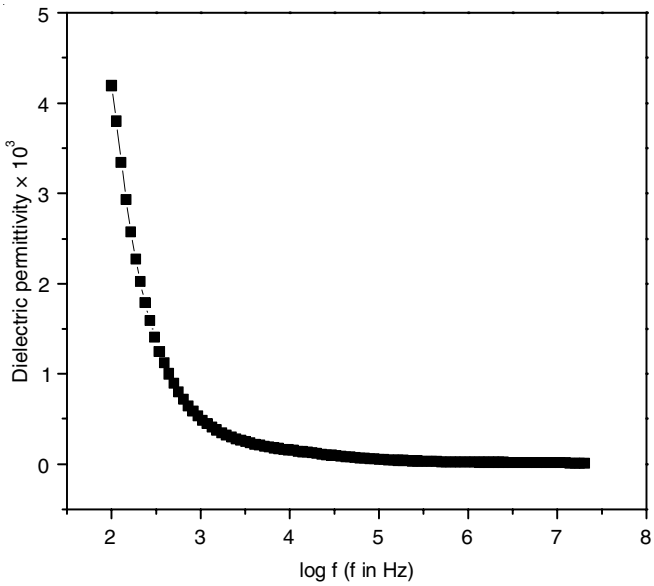

Fig. 6. Variation of dielectric permittivity of nickel ferrite with applied frequency

zation effect that occurs within the matrix. At low frequencies the total polarization in polar materials is the sum of multi components *i.e.*, deformational polarization (electronic and ionic) and relaxation (orientation and interfacial) polarization. The electronic polarization is due to the movement of valence electrons, ionic polarization is due to the movement of positive and negative ions, orientation polarization is the dipolar polarization which appears in the materials having molecules with permanent electric dipole moments capable of changing orientation into the direction of applied electric field and the interfacial polarization is due to the impedance of mobile charge carriers by interfaces. As the frequency increased the dipole cannot able to oscillate rapidly and will lag behind the applied electric filed. Thus the polarization due to orientation will not be in phase. So the dielectric permittivity decreases with the increase of the applied frequency and reaches a constant value at high frequencies [20,21]. The high value of dielectric permittivity confirms the dipolar structure of PANI matrix.

Loading dependence of dielectric permittivity of PANI-nickel ferrite composites at selected frequencies are depicted in the Fig. 8 which shows that P4N10 shows the highest value of dielectric permittivity. This may be due to the effective composite formation of 10 g nickel ferrite with 0.4 M aniline. Low value of P3N5 shows the low concentration of aniline to make coating over 10 g ferrite particles. Low value of P4N15 may be due to higher amount of ferrite.

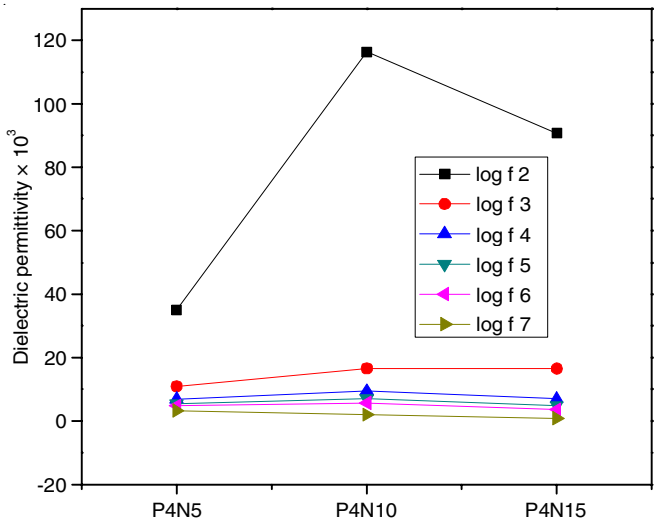

Fig. 8. Loading dependence of dielectric permittivity of PANI-nickel ferrite composites

Theoretical fitting of dielectric permittivity of PANI-$NiFe_2O_4$ nanocomposites: Several empirical equations are available in the literature which can be applied to determine the effective dielectric permittivity of two component composite systems [22]. To verify the dielectric permittivity value of composites Maxwell-Wagner mixing rule is applied and is represented in the eqn. 1 [23,24]. In this particular study the exact weight fraction of the polymer is not possible to obtain from the weight of aniline used for polymerization and chance of formation of oligomers and presence of unreacted aniline should also be considered. These molecules will be washed out during the synthesis stage. So a correction factor is included in the eqn. 1 and modified as eqn. 2:

$$\varepsilon_{eff} = \varepsilon_m \frac{\left[1 - 2V_f \frac{(\varepsilon_m - \varepsilon_f)}{(2\varepsilon_m + \varepsilon_f)}\right]}{\left[1 + V_f \frac{(\varepsilon_m - \varepsilon_f)}{(2\varepsilon_m + \varepsilon_f)}\right]} \quad (1)$$

$$\log(\varepsilon_{eff}) = \log\left(\varepsilon_m \frac{\left[1 - 2V_f \frac{(\varepsilon_m - \varepsilon_f)}{(2\varepsilon_m + \varepsilon_f)}\right]}{\left[1 + V_f \frac{(\varepsilon_m - \varepsilon_f)}{(2\varepsilon_m + \varepsilon_f)}\right]}\right) + \log k \quad (2)$$

The fitting curves corresponding to the eqns. 1 and 2 with the experimental values of the samples P4N5, P4N10 and P4N15 of PANI-nickel ferrite composites are shown in Fig. 9. It is clear from the Fig. 9 that P4N5 shows finest agreement between theoretical and observed values at higher frequencies. P4N10 and P4N15 also shows good agreement at higher frequencies with a k value ranges from 0.8 to 1.8. At low frequencies maximum contribution towards dielectric permittivity is from the interfacial and orientation polarization of PANI. Therefore small variation in the weight fraction of PANI causes large deviation at low frequencies and is observed in case of all the three samples.

Magnetic properties: Fig. 10 shows the hysteresis loop of PANI. Its saturation magnetization (Ms), magnetic remenance (Mr) and coercivity (Hc) values are 0.06, 0.01 and 231.19, respectively. PANI shows very low values of magnetic properties and can be taken as a non-magnetic material.

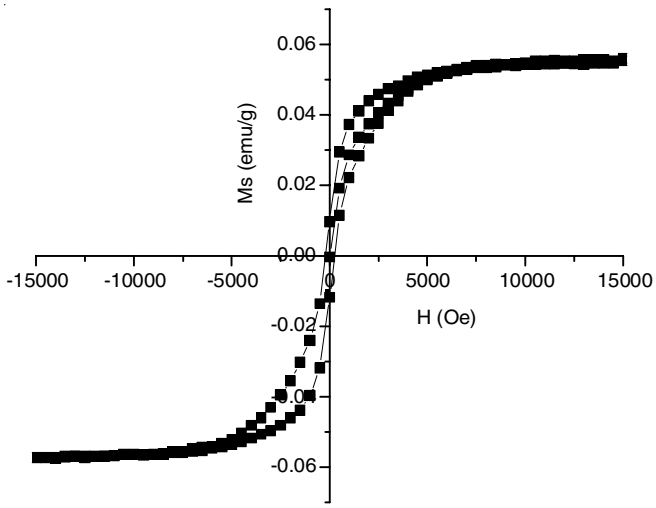

Fig. 10. Hysteresis loop of PANI

Hysteresis loop of nickel ferrite synthesized by sol-gel method is shown in the Fig. 11. The magnetic parameters Ms, Mr and Hc calculated from the loop are 38.45 emu/g, 2.74 emu/g and 74 Oe, respectively. The saturation magnetization and coercivity values of the synthesized sample are found less than that of the reported values of the bulk sample (Ms–55 emu/g and Hc–130 Oe) and may be due to the decrease in particle size which produces surface effects and causes spin disorder.

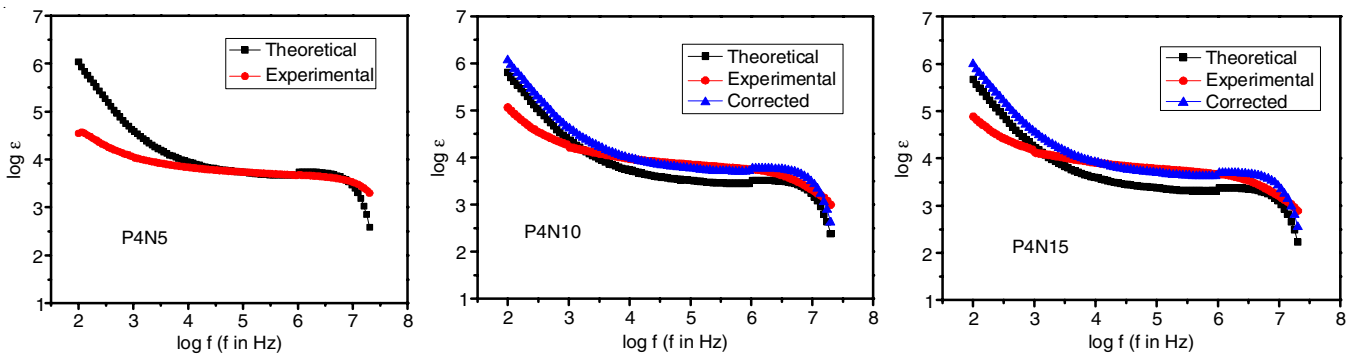

Fig. 9. Maxwell-Wagner and experimental log ε *versus* log f of PANI-nickel ferrite nanocomposites

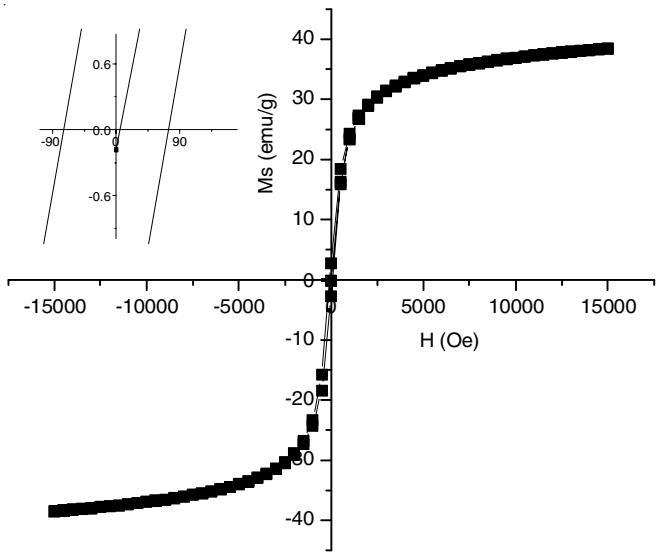

Fig. 11. Hysteresis loop of $NiFe_2O_4$

The hysteresis loops of PANI-nickel ferrite composites obtained from the VSM analysis are plotted in the Fig. 12 and the magnetic parameters are represented in the Table-1. The Ms values of the composites are lower than that of pure nickel ferrite which showing the non-magnetic coating of PANI over it. Coating of PANI over ferrite particles decrease the magnetization of ferrite in the composites and thereby decrease the magnetic properties. The Ms values of the composites are found increasing with increase in the ferrite content. Thus it is clear that magnetic properties of the PANI-ferrite composites can be varied by varying the amount of filler.

Comparison of theoretically expected Ms with the experimental Ms of PANI-$NiFe_2O_4$ composites: The decrease

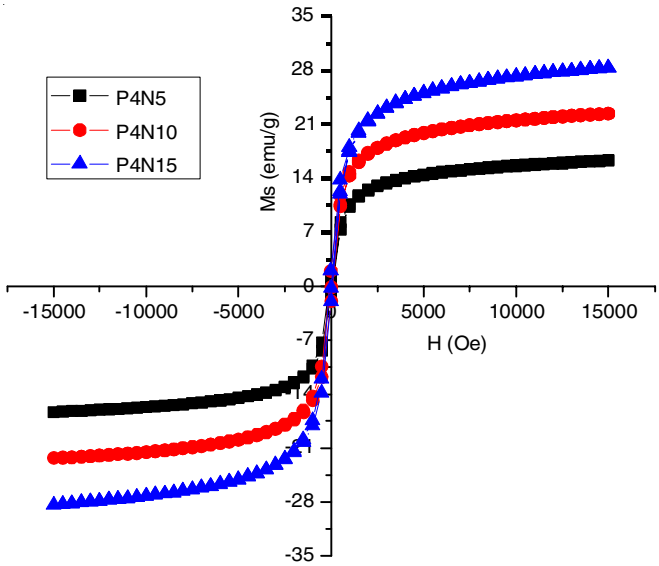

Fig. 12. Hysteresis loops of PANI-$NiFe_2O_4$ composites

TABLE-1
MAGNETIC PROPERTIES OF PANI-$NiFe_2O_4$ COMPOSITES

Sample	Ms	Mr	Hc
P4N5	16.32	1.24	72
P4N10	22.36	1.95	79
P4N15	28.35	2.01	72

in the saturation magnetization of the composites depends on the weight fraction of ferrite in the composites. The expected Ms value of the composite can be calculated by the eqn. 3:

$$Ms = W_1M_1 + W_2M_2 \quad (3)$$

where Ms is the saturation magnetization of the composite, W_1 and W_2 are the weight fractions and M_1 and M_2 are the saturation magnetizations of the ferrite and polymer, respectively. Since the polymer used for the composite preparation is non-magnetic, the modified eqn. 4, can be used to evaluate the Ms values of the composites.

$$Ms = W_1M_1 \quad (4)$$

Theoretical Ms values obtained as per the eqn. 3 and the experimental values of the PANI-nickel ferrite composites are plotted in the Fig. 13. The curve show remarkable variation between theoretical and experimental values. This may be due to the dispersion of ferrite particles in the non-magnetic PANI matrix which may resist the magnetization of ferrites. Incorporating the negative effect of PANI in the magnetization of the ferrite, the eqn. 4 can be modified as eqn. 5.

$$Ms = W_1M_1\text{-}k \quad (5)$$

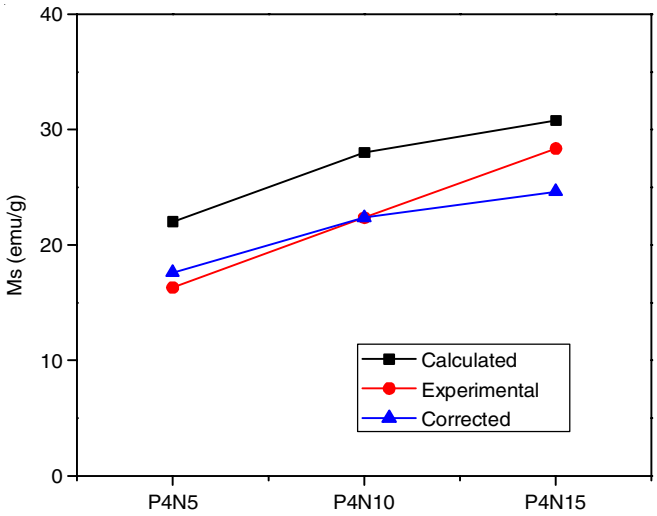

Fig. 13. Experimental, calculated and corrected Ms values of P4 series of PANI-$NiFe_2O_4$ composites

In these composites a correction factor of 16 % of the theoretical value could make an agreement of the experimental curve to the theoretical curve which is also represented in the Fig. 13. The maximum agreement is observed in 10 g composite which confirms the most effective composite formation of PANI with 10 g nickel ferrite. Higher value of P4N15 attributes the agglomerated ferrite particles due to excess weight fraction of ferrite in this sample.

Conclusion

Advances in synthetic polymer technology and nanoscience facilitate the utilization of the unique properties of conducting polymers and their composites with various materials in numerous applications. Various approaches for the manipulation of physical and chemical properties of such kind of polymer composite materials are taking wide attention of researchers. In this work PANI-nickel ferrite composites with appre-

ciable electrical and magnetic properties have been successfully synthesized in the medium of naturally available fruit extract of the plant *Tamarindus indica*. It is also found that the electrical and magnetic properties of the composites can be varied by varying the filler content. Theoretical values of dielectric and magnetic properties show good agreement with the experimental values. Thus it is concluded that the tamarind extract is an effective green medium for the synthesis of PANI-nickel ferrite composites having desired electrical and magnetic properties.

ACKNOWLEDGEMENTS

Sincere thanks extended to UGC, New Delhi, India for granting Faculty Development Programme. Thanks are also due Department of Physics, Maharajas College, Ernakulam, Department of Physics, S.D. College, Alappuzha, SAIF, IIT, Madras and SAIF, CUSAT, Cochin, India for the analysis.

CONFLICT OF INTEREST

The authors declare that there is no conflict of interests regarding the publication of this article.

REFERENCES

1. J. Stejskal and R.G. Gilbert, *Pure Appl. Chem.*, **74**, 857 (2002); https://doi.org/10.1351/pac200274050857
2. S.B. Kondawar, A.I. Nandapure and B.I. Nandapure, *J. Adv. Mater. Lett.*, **5**, 339 (2014); https://doi.org/10.5185/amlett.2014.amwc.1035
3. V.J. Babu, S. Vempati and S. Ramakrishna, *Mater. Sci. Appl.*, **4**, 1 (2013); https://doi.org/10.4236/msa.2013.41001
4. Y. Li, H. Zhang, Y. Liu, Q. Wen and J. Li, *Nanotechnology*, **19**, 105605 (2008); https://doi.org/10.1088/0957-4484/19/10/105605
5. H.G. Taleghani, M. Aleahmad and H. Eisazadeh, *World Appl. Sci. J.*, **6**, 1607 (2009).
6. J.C. Aphesteguy, P.G. Bercoff and S.E. Jacobo, *Physica B*, **398**, 200 (2007); https://doi.org/10.1016/j.physb.2007.04.018
7. G.D. Prasanna, H.S. Jayanna and V. Prasad, *J. Appl. Polym. Sci.*, **120**, 2856 (2011); https://doi.org/10.1002/app.33304
8. C.B. Sridhar, J. Husain and M.A. Prasad, *Int. J. Adv. Eng. Technol.*, **7**, 532 (2014).
9. E.E. Tanriverdi, A.T. Uzumcu, H. Kavas, A. Demir and A. Baykal, *Nano-Micro Lett.*, **3**, 99 (2011); https://doi.org/10.1007/BF03353658
10. M. Khairy and M.E. Gouda, *J. Adv. Res.*, **6**, 555 (2015); https://doi.org/10.1016/j.jare.2014.01.009
11. A.A. Syed and M.K. Dinesan, *Talanta*, **38**, 815 (1991); https://doi.org/10.1016/0039-9140(91)80261-W
12. J.-C. Chiang and A.G. MacDiarmid, *Synth. Met.*, **13**, 193 (1986); https://doi.org/10.1016/0379-6779(86)90070-6
13. G.G. Wallace, P.R. Teasdale, G.M. Spinks and A.P. Leon, Kane-Maguire, Conductive Electroactive Polymers: Intelligent Polymer Systems, Taylor and Francis: Boca Raton, edn 3 (2008).
14. A.G. MacDiarmid, J.C. Chiang, A.F. Richter and A.J. Epstein, *Synth. Met.*, **18**, 285 (1987); https://doi.org/10.1016/0379-6779(87)90893-9
15. A.H. Elsayed, M.M. Eldin, A.M. Elsyed, A.A. Elazm, E.M. Younes and H.A. Motaweh, *Int. J. Electrochem. Sci.*, **6**, 206 (2011).
16. M.A. Carvalho-Mazzeu, L.K. Faria, M.R. Baldan, M.C. Rezende and E.S. Gonçalves, *Braz. J. Chem. Eng.*, **35**, 123 (2018); https://doi.org/10.1590/0104-6632.20180351s20160201
17. E. Ozkazanc, S. Zor, H. Ozkazanc and U. Abaci, Polym. Eng. Sci., **51**, 617 (2011); https://doi.org/10.1002/pen.21866
18. R. Valenzuela, *Phys. Res. Int.*, **2012**, 1 (2012); https://doi.org/10.1155/2012/591839
19. C. Kittel, P. McEuen and P. McEuen, Introduction to Solid State Physics, vol. 8. Wiley: New York (1996).
20. S.M. Hassan, A.G. Baker and H.I. Jafaar, *Int. J. Basic Appl. Sci.*, **1**, 338 (2012); https://doi.org/10.17142/ijbas-2012.1.2.22
21. I. Sadiq, S. Naseem, M. Naeem Ashiq, M.A. Khan, S. Niaz and M.U. Rana, *Progr. Nat. Sci.: Mater. Int.*, **25**, 419 (2015); https://doi.org/10.1016/j.pnsc.2015.09.011
22. P. Barber, S. Balasubramanian, Y. Anguchamy, S. Gong, A. Wibowo, H. Gao, H. Ploehn and H.-C. Zur Loye, *Materials*, **2**, 1697 (2009); https://doi.org/10.3390/ma2041697
23. K.W. Wagner, *Arch. J. Elektrotech*, **2**, 371 (1914); https://doi.org/10.1007/BF01657322
24. D.-H. Yoon, J. Zhang and B.I. Lee, *Mater. Res. Bull.*, **38**, 765 (2003); https://doi.org/10.1016/S0025-5408(03)00075-8